# Advancing Beyond Charge Analysis Using the Electronic Localization Function: Chemically Intuitive Distribution of Electrostatic Moments

**JULIEN PILMÉ,[1,2] JEAN-PHILIP PIQUEMAL[2]**

[1]*Faculté de pharmacie, Université de Lyon, Université Lyon 1, F-69373 Lyon, Cedex 08, France*
[2]*Laboratoire de Chimie Théorique, UMR 7616 CNRS, Université Pierre et Marie Curie, Paris 6, Case Courier 137, 4 place Jussieu, 75252 Paris Cedex 05, France*

**Abstract:** We propose here an evaluation of chemically intuitive distributed electrostatic moments using the topological analysis of the electron localization function (ELF). As this partition of the total charge density provides an accurate representation of the molecular dipole, the distributed electrostatic moments based on the ELF partition (DEMEP) allows computing of local moments located at non atomic centers such as lone pairs, $\sigma$ bonds and $\pi$ systems. As the local dipole contribution can be decomposed in polarization and charge transfer components, our results indicate that local dipolar polarization of the lone pairs and chemical reactivity are closely related whereas the charge transfer contribution is the key factor driving the local bond dipole. Results on relevant molecules show that local dipole contributions can be used to rationalize inductive polarization effects in alcohols derivatives and typical hydrogen bond interactions. Moreover, bond quadrupole polarization moments being related to a $\pi$ character enable to discuss bond multiplicities, and to sort families of molecules according to their bond order. That way, the nature of the C—O bond has been revisited for several typical systems by means of the DEMEP analysis which appears also helpful to discuss aromaticity. Special attention has been given to the carbon monoxide molecule, to the CuCO complex and to a weak intramolecular N|---CO interaction involved in several biological systems. In this latter case, it is confirmed that the bond formation is mainly linked to the CO bond polarization. Transferability tests show that the approach is suitable for the design of advanced force fields.

© 2008 Wiley Periodicals, Inc.    J Comput Chem 29: 1440–1449, 2008

**Key words:** distributed multipoles; electron localization function; topological analysis; bonding analysis

## Introduction

Through years many studies have been devoted to the evaluation of distributed moments. Following the pioneer work by Stone[1–3] and Claverie,[4] several groups have proposed atom centered multipole extraction methods based on a partition of the total charge density[5–7] or on the fitting of the moments to the molecular electrostatic potential (MESP).[8–10] Among these approaches Bader[11,12] and Popelier[13] proposed to compute atomic moments using a partition of the total charge density grounded on the topological analysis of the electron density, the so-called atoms in molecules theory (AIM).[11] These approaches have been successfully applied to molecular modeling since new generation force fields[14–19] have taken advantage of these more elaborate representations of the total charge distribution. Nevertheless, these methods (at the exception of AIM) provide limited chemical information as they aim to reproduce electrostatic potential. Moreover, it has been noticed[1–5,13a] that an accurate representation of

the potential requires high-rank atomic multipole moments, typically up to hexadecapole. Another strategy suggested by Claverie[4b] showed that a same order of accuracy can be obtained using a multipole expansion limited to quadrupoles if distributed moments on several non atomic extra sites such as bonds midpoints are added. Indeed, an improved reproduction of the ab initio molecular electrostatic potential was also observed by Stone,[1–3] Soderhjelm et al.,[6a] and Cisneros et al.,[7] by adding extra points. Such assumption can be refined by noticing that significant increase of the accuracy can be obtained by choosing a position different from the midpoint location by considering for example the bond barycenter of charges[4] or the centroid of the bond localized orbital.[6a,7] However, to add chemical signifi-

*Correspondence to:* J. Pilmé; UPMC Univ Paris 06, UMR 7616, Laboratoire de Chimie Théorique, case courier 137, 4 place Jussieu, F-75005, Paris, France; e-mail: pilme@lct.jussieu.fr or J.-P. Piquemal; e-mail: jpp@lct.jussieu.fr

cance, such extra sites should not be restricted to bonds and should also ideally be located on lone pairs. At this point, the GEM[7] methodology remains the only methodology enabling a projection of moments on any non atomic centers. Nevertheless, their localization is not computed by the approach and requires external informations (orbital localization etc...).

On a theoretical point of view, the crucial relationship of lone pairs to the molecular dipole has been extensively studied for water (see ref. 20a and references therein) and has been recently illustrated by a tutorial study[20b] dedicated to the carbon monoxide molecule. The authors have pointed out the fundamental role of the dipolar contribution of the frontier orbital $7\sigma$, traditionally interpreted as the carbon lone pair, to the molecular dipole and to the reactivity of that species as a nucleophilic entity. This example shows that localized higher moments could constitute far more interesting descriptors than the usual atom-centered charges generally used by chemists to rationalize electronic structures.

The purpose of this contribution is to propose an integrated first principles approach to access the local value of moments beyond atomic centers and to expand on the work of Bader and Popelier by using a topological analysis. To do so, we propose to use a nonarbitrary partition based on the topological analysis of the electron localization function (ELF) of Becke and Edgecombe.[21,22] After a presentation of the methodology, we will present an application the distributed electrostatic moments relying on the ELF partition (DEMEP) to several molecules and complexes, including several species molecules involved in H bonding such as the water dimer, a set of several carbonyl bonds in different chemical environments, an unusual intramolecular N|—CO bond interaction as well as the CuCO complex. As the monopole term, i.e., the ELF (or AIM) population, has been widely discussed in the literature, we will focus on higher-order terms.

## Theory

### *The ELF Function and Its Topological Analysis*

In a topological analysis, a partitioning of the molecular space is achieved by the theory of gradient dynamical systems. This partitioning gives a set of molecular volumes or regions (the so-called "basins" denoted as $\Omega$) localized around maxima (attractors) of the vector field of a scalar function V(**r**). The frontier between each basin is then a zero-flux surface satisfying the following condition for every point **r** on the surface: $\nabla$V(**r**). **n** = 0, **n** being the unit vector normal to the surface. In the "Atoms in Molecule" theory of Bader,[11] this scalar function is the electron density and the basins are associated to the atoms belonging to the molecule. However, for over a decade, the topological analysis of the ELF[21,22] has been extensively used for the analysis of chemical bonding as well for investigating chemical reactivity.[23–33] Indeed, the ELF function can be interpreted as a signature of the electronic-pair distribution.[24] The relationship of the ELF function to pair functions has been demonstrated but, in contrast to these latter, ELF is defined to have values restricted between 0 and 1 and so can be easily calculated and interpreted. Once computed on a 3D grid, the ELF function can be partitioned into an intuitive chemical scheme. Indeed, core regions

can be determined (if $Z > 2$) for any atom A, the core basin being labeled C(A). Regions associated to lone pairs are labeled V(A) and bonding region denoting chemical bonds are noted V(A,B), in contrast to the AIM theory[11] where the basins are localized on atoms only. These ELF regions match closely the domains of the VSEPR model.[34,35] Computational cost is essentially the same as for AIM.[11a]

### *Topological Moments*

The population of a basin can be calculated by integrating the one-electron density over the basin volume and corresponds, in the framework of a distributed moments analysis, to the opposite of the monopole term, $M_0(\Omega)$:

$$M_0(\Omega) = - \int_\Omega \rho(\mathbf{r})d\tau \tag{1}$$

Some years ago, a way to compute the local electrostatic moments have been proposed in the framework of the AIM theory by Bader et al.,[12b] and latter improved and generalized to higher moments by Popelier et al.,[13] As seen above, the mathematical properties of the electron density do not allow the determination of nonatomic attractors and so of nonatomic moments but the ELF function allows accessing such quantities. That way, the initial formalism used in the AIM theory for the determination of atomic basin moments can be easily adapted to the ELF partition as follows.

The first moments or dipolar polarization components of the charge distribution are defined by 3D integrals for a given basin $\Omega$ as:

$$M_{1,x}(\Omega) = - \int_\Omega (x - X_c)\rho(\mathbf{r})d\tau$$

$$M_{1,y}(\Omega) = - \int_\Omega (y - Y_c)\rho(\mathbf{r})d\tau \tag{2}$$

$$M_{1,z}(\Omega) = - \int_\Omega (z - Z_c)\rho(\mathbf{r})d\tau$$

where $X_c$, $Y_c$, $Z_c$ are the cartesians coordinates of the basins centers.

In most cases, the valence basin center is located at the attractor position. It is important to note that the attractor's position is not arbitrary but defined by the mathematical properties of the ELF function in the framework of the theory of dynamical systems. In the case of bonds, attractors do not systematically localized on the bond midpoint and their localization depends on electronegativity differences between the atoms forming the bond and on the nature of the chemical environment. For example, the C—C bond attractor of the ethane molecule is the bond midpoint while the C—O bond attractor of a $CH_3OH$ molecule is closer to the oxygen atom. In the case of lone pairs, the positions of the attractors are generally in agreement with the qualitative domains positions predicted by the

VSEPR model. For circular valence attractors such as for the C—C bond present in the ethyne molecule, the $X_c$, $Y_c$, $Z_c$ positions will be chosen as the center of the basin volume defining the 3D toric basin.

In the same spirit, the five second-moment spherical tensor components are defined as the quadrupolar polarization terms and are the ELF basin equivalent to the atomic quadrupoles moments introduced by Popelier[13a] in the case of an AIM analysis:

$$M_{2,zz}(\Omega) = -\frac{1}{2} \int_\Omega \left( 3(z - Z_c)^2 - \mathbf{r}^2 \right) \rho(\mathbf{r}) d\tau$$

$$M_{2,x^2-y^2}(\Omega) = -\frac{\sqrt{3}}{2} \int_\Omega \left[ (x - X_c)^2 - (y - Y_c)^2 \right] \rho(\mathbf{r}) d\tau$$

$$M_{2,xy}(\Omega) = -\sqrt{3} \int_\Omega (x - X_c)(y - Y_c) \rho(\mathbf{r}) d\tau \qquad (3)$$

$$M_{2,xz}(\Omega) = -\sqrt{3} \int_\Omega (x - X_c)(z - Z_c) \rho(\mathbf{r}) d\tau$$

$$M_{2,yz}(\Omega) = -\sqrt{3} \int_\Omega (y - Y_c)(z - Z_c) \rho(\mathbf{r}) d\tau$$

The first or second moment basin magnitude is then defined as the square root of the sum of squared components:

$$|\mathbf{M}(\Omega)| = \sqrt{\sum_i M_i(\Omega)^2}$$

Thanks to the invariance of magnitude of any multipole rank ($|\mathbf{M}_1|$ or $|\mathbf{M}_2|$) with respect to the axis for a given bond or lone pair,[36,13a] the approach should allow us to compare the dipolar or quadrupolar polarization of such lone pair in different chemical environments.

### *Molecular Dipole*

Following the ELF partition, the static molecular dipole $\mu$ is expressed in terms of a sum of the local dipole contributions over all $\Omega$ basins (core and valence):

$$\mu = \sum_\Omega \mu_{\text{valence}}(\Omega) + \sum_\Omega \mu_{\text{core}}(\Omega) \qquad (4)$$

$\mu_{\text{valence}}(\Omega)$ is the local dipole contribution of a given valence basin and $\mu_{\text{core}}(\Omega)$ is the local dipole contribution of a given core basin. As noted by Coulson[37] and Bader et al.,[12] the dipole contributions can not reasonably be related to the sole charge transfer terms as the electron density is not spherically distributed in the basin's volume. Thus, the dipole contribution takes into account the dipolar polarization of the charge density through the first moment ($\mathbf{M}_1$). $\mu_{\text{valence}}(\Omega)$ is then split into a dipolar polarization $\mathbf{M}_1$ (first moments) and into an electronic charge transfer term expressed as follows:

$$\mu_{\text{valence}}(\Omega) = \mathbf{M}_1(\Omega) + \mathbf{M}_0(\Omega)\mathbf{X}_\Omega \qquad (5)$$

where $\mathbf{X}_\Omega$ is the position vector of the ELF basin center from some arbitrary origin.

Similarly, $\mu_{\text{core}}(\Omega)$ is split into polarization ($\mathbf{M}_1$) and two charge transfer terms namely electronic and nuclear as given bellow:

$$\mu_{\text{core}}(\Omega) = \mathbf{M}_1(\Omega) + \mathbf{M}_0(\Omega)\mathbf{X}_\Omega + Z.\mathbf{X}_\Omega \qquad (6)$$

$Z$ is the atomic number and $\mathbf{X}_\Omega$ is then the nuclear position.

In contrast to $M_1$ and its magnitude (see Topological Moments paragraph of this section), the individual contributions of the charge transfer and consequently, the dipole contribution $\mu(\Omega)$ (sum of $M_1$ and charge transfer terms) depend of the origin choice but their sum does not. Therefore, in order to compare the magnitude of the local dipole contribution of functional groups in related systems, we have to define a local coordinates system, i.e. the "local frame" which is common to the compared molecules. Local frames definitions are given in captions of Tables (see for example Tables 3 and 5). For a given coordinate system, the magnitude of the dipole contribution for any valence basin (bond or lone pair) stays invariant under molecular rotation and thus, appears as a useful tool for the rationalization of electronic structures.

## Computational Methods

All Geometries have been optimized using the hybrid functional B3LYP[38,39] with the Gaussian 2003 software.[40] The standard all-electron basis set 6-311G(3d) was employed. (Basis sets were obtained from the Extensible Computational Chemistry Environment Basis Set Database, Version 02/02/06, as developed and distributed by the Molecular Science Computing Facility, Environmental and Molecular Sciences Laboratory which is part of the Pacific Northwest Laboratory, P.O. Box 999, Richland, Washington 99352, USA, and funded by the U.S. Department of Energy). All the topological analyses were carried out using ELF grids of size $130 \times 130 \times 130$ with a modified version of the TopMoD package.[41] Numerical integrations of the electron density over basin volumes have been carried out using the same modified code. Constrained space orbital variations (CSOV)[42] intermolecular energy decompositions were performed at the same level of theory using an in-house version[43] of HONDO 93.5.[44] To compute the total molecular dipole, we have assumed as "global (or molecular) frame" the standard orientation of Gaussian 2003, which computes the molecular dipole at the center of nuclear charges.

## Results and Discussion

To test the accuracy of our method, we have tested our code[41b] by computing molecular dipoles and by comparing their values to comparisons to their Gaussian 2003 ab initio reference. Moreover, using an AIM partition, our results compare satisfactorily to the literature data extracted from previous studies.[13,16] For example, our AIM calculations reproduce accurately the molecular dipole of a single water molecule (1.860 Debye) with respect to the reference ab initio value (1.859 Debye) obtained at the B3LYP/6-311G(3d). Table 1 shows that the magnitudes of the first and second local AIM moments for each atom involved in the single water molecule are in excellent agreement with the previous calculation given in the literature.[16a]

**Table 1.** Magnitudes of First and Second Local AIM Moments.

| Atoms | $X^a$ | $Y^a$ | $Z^a$ | $Q^b$ | $|M_1|^c$ | $|M_2|^c$ | $|\mu|^d$ |
|---|---|---|---|---|---|---|---|
| Water molecule | | | | | | | 1.860 (1.859) |
| O | 0.00 | 0.00 | 0.12 | −1.16 (−1.21)[e] | 0.36 (0.40)[e] | 0.64 (0.68)[e] | |
| H1 | 0.00 | 0.75 | −0.48 | 0.58 (0.61)[e] | 0.16 (0.17)[e] | 0.02 (0.04)[e] | |
| H2 | 0.00 | −0.75 | −0.48 | 0.58 (0.61)[e] | 0.16 (0.17)[e] | 0.02 (0.04)[e] | |
| Water dimer | | | | | | | 1.973 (1.909) |
| O (acceptor) | 0.00 | 0.00 | 0.00 | −1.12 | 0.29 | 0.70 | |
| H1 | 0.00 | 0.00 | 0.97 | 0.58 | 0.13 | 0.04 | |
| H2 | 0.94 | 0.00 | −0.22 | 0.54 | 0.16 | 0.01 | |
| O (donor) | −0.36 | −0.01 | 2.85 | −1.12 | 0.31 | 0.73 | |
| H3 | −0.94 | −0.78 | 2.84 | 0.58 | 0.15 | 0.01 | |
| H4 | −0.98 | 0.72 | 2.85 | 0.58 | 0.15 | 0.01 | |

[a]Nuclear coordinates (Angstrom).
[b]AIM Atomic charges Q (electron).
[c]Magnitude of the AIM First $|M_1|$ and Second atomic $|M_2|$ moments (au) optimized at the B3LYP/6-311G(3d) level.
[d]AIM Molecular Dipole in Debye and, in parenthesis, its ab initio reference value.
[e]In parenthesis, comparative AIM values from Literature as given in ref. 16a.

### *A Step Beyond Charge: Use of the Local Dipolar Polarization*

Table 2 presents the reconstructed and reference ELF molecular dipole for a set of various covalent or dative molecules such as $H_2O$, $CH_3OH$, glycine, CO, and $BH_3NH_3$, as well as LiH, a typical ionic compound. The canonical water dimer and the $Cl(H_2O)^-$ complex were studied as typical systems involving an hydrogen bond. Magnitude of the dipolar polarization $|M_1|$ and local dipole contributions of some bonds and lone pairs of interest are also reported.

These results lead us to the following conclusions:

1. Overall, as can be seen on Table 2, the calculated molecular dipoles are in excellent agreement with the reference ab initio calculation. As expected, the local charge transfer terms $\mu_{CT}$ and the polarization terms $M_1$ are found in opposite direction.[12,45]

2. According to the chemical intuition, the core basins provide a near-null dipolar polarization term while the valence basins, i.e., the bonding and nonbonding regions, displays significant contributions. For example, the dipolar polarization magnitude of the nitrogen core in $N_2$ is lower than $10^{-2}$ a.u.

3. Local polarization of the lone pairs should ideally be related to the chemical reactivity. For example, the relative reactivity of the carbon and oxygen lone pairs in the carbon monoxide (CO) is still debated.[20b] Figure 1 displays the ELF localization domains of the CO molecule. This figure shows that the valence is split in three basins i.e., bonding V(C,O) and the two lone pairs, one on each atoms denoted V(C) and V(O).

That way, the local dipole contributions of the carbon and oxygen lone pairs are denoted $\mu(V(C))$ and $\mu(V(O))$. They were found to be in opposite direction and their magnitude to be about 4.8 and 5.4 a.u. respectively. This result means that the both lone pairs have a comparable and significant role for the chemical behaviour of the CO molecule. Moreover, the result indicates their quite similar contributions to the total

molecular dipole. In that case, this last point contradicts the usual chemical intuition based on the electronegativity differences which predicts a major contribution of the oxygen to the molecular dipole. A more in depth-study of the electronic structure of the CO molecule is given in the next Section.

Another example can be found with the canonical water dimer. Since the first work of Morokuma and Pedersen[45] the water dimer has been the subject of intense studies (ref. 46 and references therein): Table 1 shows the first and second AIM moments for each atom involved in the dimer. As expected, these values show that the two water molecules are non equivalent because of a consequent polarization effect coupled to a small charge transfer from the donor water to the acceptor water molecule (ref. 37, 44 and references therein). In contrast to the AIM theory, the ELF topology allows to separate core and valence regions. Indeed, Figure 1 shows the localization domains of the water dimer, in particular the spatial distribution of the oxygen lone pairs V(O). Thus, the components of the molecular dipole of each individual water (see Table 2) has been computed as the sum of all local dipole components of each basin: core C(O), lone pairs V(O) and bonding V(O, H). The magnitude of the molecular dipole $|\mu|$ of each individual water molecule was found to be about 2.09 D for the donor and about 2.06 D for the acceptor, which is, in both cases, significantly larger than in the isolated monomer (1.860 D).[16,46,47] This effect can also be observed with the calculated polarization magnitude $|M_1(V(O))|$ of the lone pairs basins. This quantity appears larger in the dimer than in the single monomer but differs for each lone pair in the acceptor water. Indeed, the polarization magnitude of the lone pair involved in the hydrogen bond (acceptor water) is enhanced (0.998 a.u.) by comparison to the other lone pair (0.928 a.u.). On the contrary, both lone pairs of the donor water appear similarly polarized with a value of 0.951 a.u. for $|M_1|$. As the origin of the polarization enhancement can be understood through a deep intramolecu-

**Table 2.** Molecular Dipole Components in Debye (eq. 4).

| Molecule Basin | $-M_0$ | $\|\mathbf{M}_1\|$ | $\mu_x$[a] | $\mu_y$[a] | $\mu_z$[a] | $\|\mu\|$ |
|---|---|---|---|---|---|---|
| $H_2O$ | | | 0.0 (0.0) | 0.0 (0.0) | 1.860 (1.859) | 1.860 (1.859)[a] |
| V(O,H) | 1.58[b] | 0.675[c] | | | | 0.385[d] |
| V(O) | 2.36[b] | 0.903[c] | | | | 1.948[d] |
| $(H_2O)_2$ | | | −0.573 (−0.561) | −0.052 (−0.053) | 1.887 (1.824) | 1.973 (1.909)[a] |
| $H_2O$ (donor) | | | 1.475 | 0.00 | 1.475 | 2.09[a] |
| V(O) | 2.37[b] | 0.951[c] | | | | 1.979[d] |
| $H_2O$ (acceptor) | | | −2.020 | −0.046 | 0.419 | 2.06[a] |
| V(O) | 2.15[b] | 0.928[c] | | | | 1.873[d] |
| | 2.51[b] | 0.998[c] | | | | 1.971[d] |
| $Cl(H_2O)^-$ | | | −0.963 (−0.953) | 0.0 (0.0) | −2.134 (−2.133) | 2.341 (2.336)[a] |
| $NH_3$ | | | 0.812 (0.805) | −1.334 (−1.129) | 0.635 (0.634) | 1.530 (1.530)[a] |
| V(N) | 2.31[b] | 1.231[c] | | | | 2.074[d] |
| $N_2$ | | | | | | |
| V(N) | 3.16[b] | 2.632[c] | | | | 4.980[d] |
| V(N, N) | 3.47[b] | 0.0[c] | | | | 0.0[d] |
| $CH_3OH$ | | | 1.344 (1.342) | 0.727 (0.735) | 0.00 (0.00) | 1.528 (1.530)[a] |
| Glycine | | | −1.090 (−0.993) | 1.345 (1.332) | 1.106 (0.992) | 2.060 (1.934)[a] |
| $BH_3NH_3$ | | | 2.647 (2.671) | −4.128 (−4.168) | 1.949 (1.968) | 5.276 (5.328)[a] |
| CO | | | 0.0 (0.0) | 0.0 (0.0) | 0.146 (0.144) | 0.146 (0.144)[a] |
| V(C) | 2.59[b] | 2.841[c] | | | | 4.841[d] |
| V(O) | 4.07[b] | 2.919[c] | | | | 5.386[d] |
| V(C, O) | 3.14[b] | 0.329[c] | | | | 0.011[d] |
| LiH | | | 0.0 (0.0) | 0.0 (0.0) | 5.738 (5.747) | 5.738 (5.747)[a] |

[a]The reference ab initio values provided by the Gaussian 2003 software are given in parenthesis.
[b]Basin population (electron).
[c]Magnitude of dipolar polarization ($\|\mathbf{M}_1\|$) (a.u.).
[d]Total dipolar contribution (a.u.) for some basins (eq. 4).

lar reorganisation of the density within each water molecule due to presence of the other molecule,[13c] these results correlate very well with data extracted from a CSOV energy decomposition analysis. We can see that the polarization energy is clearly larger for the donor acceptor molecule
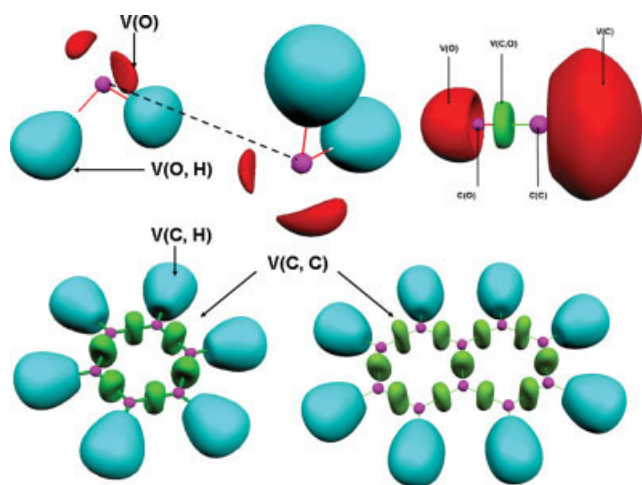


**Figure 1.** ELF localization domains for the dimer water (top, left), the benzene (bottom, left), napthalene (bottom right) and carbon monoxide (top, right). Color code: magenta, core; green, bond; light blue, C—H, and O—H bond; red, lone pair.

(−0.49 vs. −0.32 kcal/mol) linking directly the observation of local dipoles to intermolecular interactions.

4. The local dipolar polarization of a homonuclear covalent bond such as the N-N bond involved in the diatomic $N_2$ molecule, is null whereas the nitrogen lone pairs, denoted V(N), appear very polarized ($\|\mathbf{M}_1\| = 2.632$ a.u.). In contrast, the

**Table 3.** Substituant Effect on the Dipolar Polarization of the Bonding Basin V(C, O).

| Molecule | $r_{CO}$[a] | V(C, O) | | |
|---|---|---|---|---|
| | | $-M_0$[b] | $\|\mathbf{M}_1\|$[c] | $\|\mu V(C, O)\|$[d] |
| $CH_3OH$ | 1.423 | 1.23 | 0.099 | 1.573 |
| $MeCH_2OH$ | 1.425 | 1.23 | 0.097 | 1.574 |
| $(NH_2)CH_2OH$ | 1.421 | 1.27 | 0.098 | 1.636 |
| $(OH)CH_2OH$ | 1.406 | 1.33 | 0.105 | 1.700 |
| $CH_2FOH$ | 1.395 | 1.36 | 0.101 | 1.746 |
| $CF_3OH$ | 1.345 | 1.65 | 0.074 | 2.175 |
| $ClCH_2OH$ | 1.397 | 1.31 | 0.086 | 1.699 |
| $BrCH_2OH$ | 1.396 | 1.30 | 0.083 | 1.682 |

The common referential was centered on the oxygen atom.
[a]B3LYP/6-311G(3d) optimized distance in Angstrom.
[b]Basin population (electron).
[c]Magnitude of first moments (a.u.).
[d]Dipolar contribution (Debye) for some basins (eq. 4).

dipolar polarization magnitude of heteronuclear bonds can be non negligible, but the charge transfer components remain generally the main contributions to the local bond dipole contribution. For example, the CO bond in the formaldehyde molecule ($H_2CO$) displays only one polarization component ($\mathbf{M}_{1,y} = -0.151$ a.u) which is largely compensated by the charge transfer component ($\mu_{CT,y} = 0.381$ a.u.). Indeed, Table 3 shows the substituant effect on the polarization and on the dipole contribution (polarization and charge transfer) of a C—O covalent bond in several $CH_2X$—COH compounds with X = H, $CH_3$, $NH_2$, OH, F, $CF_3$, Cl, Br.[48]

These results show that the magnitude of the C—O bond polarization is quite constant for the different compounds. Nevertheless, the magnitude of the local dipole of the V(C, O) basin supports the chemical intuition based on the electronegativity differences between atoms since this magnitude can be directly correlated to the C—O distance as it has been noted for the V(C, O) basin population.[24] In other words,

these results indicate that the charge transfer term is the key factor driving the local dipole of the CO bond.[16b]

On the contrary, it is not obvious to correlate the dipole magnitude of the oxygen lone pair to the electronegativity of the substituant group because other electronic factors such as intramolecular dispersion has an effect on the total dipole.[49]

### *Local Quadrupolar Polarization*

At this stage, we propose to focus our analysis on the C—O bond which plays a fundamental role in many systems.[50] Table 4 gathers the magnitude of the quadrupolar polarization $|\mathbf{M}_2|$ of the C—O bonding basin V(C, O) together with the dipolar polarization $|\mathbf{M}_1|$ of the oxygen lone pairs for several typical carbonyl compounds. The molecules have been classified in Table 4 according to their formal C—O Bond Order (BO).

Indeed, Holt et al.,[6c] with their bond capacitance model based on Mulliken charges have shown that it was possible to perform such ranking. Moreover, Popelier[13] has shown that the

**Table 4.** Population, First, and Second Moments Contributions (a.u.) of the C—O Bond Involved in Various Chemical Environment.

| Molecule | BO[a] | $r_{CO}$[b] | V(C, O) $-M_0$ | V(C, O) $\|\mathbf{M}_2\|$ | V(O) $-M_0$ | V(O) $\|\mathbf{M}_1\|$ | $\|\mu\|$ (D)[c] |
|---|---|---|---|---|---|---|---|
| $CH_3OH$ | 1 | 1.418 | 1.25 | 0.084 | 2.39 × 2 | 0.915 | 1.528 (1.530) |
| $(CH_3)_2O$ | 1 | 1.409 | 1.30 | 0.104 | 2.41 × 2 | 0.972 | 1.121 (1.125) |
| $CO_3^{2-}$ | 1.3 | 1.306 | 1.84 | 0.563 | 3.00 × 3 | 1.043 | 0.0 (0.0) |
| $HCO_2^-$ | 1.5 | 1.250 | 2.02 | 0.750 | 2.83 × 2 | 0.998 | 2.895 (2.917) |
| $\phi$-OH | 1 | 1.364 | 1.48 | 0.095 | 2.29 × 2 | 1.361 | 1.280 (1.253) |
| $C_7$-$H_6O$ (p-quinone methide) | 2 | 1.219 | 2.25 | 1.269 | 2.66 × 2 | 1.026 | 4.451 (4.463) |
| HCOOH | 1 | 1.349 | 1.61 | 0.165 | 4.430 | 3.653 | 3.756 (3.767) |
|  | 2 | 1.189 | 2.48 | 1.291 | 2.59 × 2 | 1.138 |  |
| $NH_2COH$ | 2 | 1.207 | 2.31 | 1.156 | 2.78 × 2 | 1.195 | 3.716 (3.709) |
| $NH_3COH^+$ | 2 | 1.163 | 2.69 | 1.491 | 2.46 × 2 | 1.130 | 6.992 (7.086) |
| $H_2CO$ | 2 | 1.197 | 2.42 | 1.602 | 2.54 × 2 | 0.997 | 2.171 (2.173) |
| Glycine | 1 | 1.349 | 1.58 | 0.192 | 4.46 | 3.849 | 1.898 (1.920) |
|  | 2 | 1.206 | 2.18 | 1.205 | 2 × 2.65 | 1.010 |  |
| $HCO^+$ | 2 | 1.101 | 3.53 | 1.183 | 4.03 | 3.141 | 1.210 (1.221) |
| $N(Me)_3H_2CO$ Short[d] $H_2CO$ | 2 | 1.277 | 1.71 | 0.423 | 2.98 × 2 | 1.118 | 6.903 (6.999) 4.809[e] |
| Long[d] $H_2CO$ | 2 | 1.215 | 2.31 | 1.431 | 2.61 × 2 | 0.944 | 2.906 (2.949) 2.567[e] |
| FHCO | 2 | 1.175 | 2.58 | 1.363 | 2.56 × 2 | 1.171 | 1.985 (1.968) |
| CO | 3 | 1.125 | 3.14 | 0.902 | 4.07 | 2.919 | 0.146 (0.144) |
| $CO^-$ | 2.5 | 1.223 | 2.18 | 0.727 | 2.54 × 2 | 1.052 | 1.964 (1.968) |
| $CO_2$ | 2 | 1.159 | 3.03 | 0.730 | 4.79 | 3.700 | 0.0 (0.0) |
| CuCO($^2$A') | 2 | 1.144 | 2.85 | 0.784 | 4.41 | 3.389 | 1.081 (1.131) |
| CuCO($^2\sum^+$) | 2 | 1.131 | 3.08 | 0.841 | 4.30 | 3.163 | 0.470 (0.438) |

[a]Formal bond order of the C—O bond.
[b]B3LYP/6-311G(3d) optimized distance (in Angstrom), except for $N(Me)_3H_2CO$ optimized at the B3LYP/6-31+G(d) level.
[c]Molecular Dipole components in Debye (eq. 3) The exact ab initio values provide by the Gaussian software are given in parenthesis.
[d]N—CO long distance regime ($r_{NC}$ = 3.00 Å) and N—CO short distance regime ($r_{NC}$ = 1.63 Å).
[e]AIM dipolar contribution of the $H_2CO$ fragment (Debye).

**Figure 2.** Magnitude of quadrupolar polarization $|M_2|$ (au.) for carbonyl derivatives as a function of the C—O distance (Å). The two dashed lines correspond to the transitions in formal CO bond order.

magnitude of the AIM quadrupolar polarization is linked to the $\pi$ population of a bond.

However, if the AIM theory is able to provide atomic quadrupolar magnitude, the separation between bonding and nonbonding (lone pairs) contributions remains confuse. As illustrated in Figure 2, the quadrupolar magnitude allows rationalizing the multiplicity order of the C—O bond.

Indeed, large values of $|M_2|$ can be connected to a strong $\pi$ bond character such as in $H_2CO$ ($|M_2|$ = 1.602 a.u.) while an interaction dominated by the $\sigma$ contributions shows a very weak value of $|M_2|$ as in $CH_3OH$ (0.084 a.u.). Consequently, we observe widespread intermediates values for known systems exhibiting a $\pi$ delocalization character such as in $CO_3^{2-}$ ($|M_2|$ = 0.563 a.u.). Similar conclusions can be given for molecules involving C—C bonds (not reported in Table 4). Figure 1 displays the ELF localization domains of the benzene and naphthalene molecules. The figure shows identical V(C, C) bonding basins as expected for the aromatic systems.[32] Similarly to the carbonyl systems, the quadrupolar polarization of the V(C, C) basin increases for the sequence $C_2H_6$ (0.973 a.u.), benzene (2.00 a.u.), naphtalene (2.769 a.u. for the double bond and 1.448 for the single bond) and $C_2H_2$ (2.865 a.u.) as a function of the $\pi$ character. We must note that the evaluation of the polarization for systems exhibiting two symmetrical bonding basins above and bellow the molecular plane such as $C_2H_4$ is not obvious due to several basin centers possible definitions.

### *Revisiting Carbon Monoxide: CO Versus HCO+*

The case of the CO molecule is particularly interesting because its bonding nature is still subjected to intense theoretical discussions. Recently, Frenking et al.,[20b] have demonstrated that the dipole contribution of the HOMO $7\sigma$ molecular orbital, traditionally assigned to the C lone pair, must be considered to understand the chemical properties of the molecule as well as to calculate a significant value of the total dipolar moment. Moreover, the authors have demonstrated that the $\pi$ contributions and

$\sigma$ contributions are expected to be almost equivalent in the bond. Our value of 0.902 a.u. (see Table 3 and Fig. 2) for the quadrupolar polarization of the carbonyl bond indicates that the $\pi$ contribution is weaker in comparison to other $\pi$ systems such as $HCO^+$. As previously explained, the values of the local dipole magnitude of both lone pairs are respectively found similar (see Table 2). These results confirm the relative equivalence of both lone pairs for the chemical behavior of the CO molecule. Moreover, it is possible to characterize the nucleophilic character of the carbon lone pair by a positive point charge $Q^+$ located near to the carbon atom (1 Å).[20b] Indeed, under the charge effect, the two lone pairs become similar: the dipole of the carbon lone pair increases to 5.1 a.u. while the dipole of the oxygen lone pair is simultaneously decreased to 5.1 a.u. The quadrupolar polarization of the $Q^+$-C-O bond becomes 1.167 a.u., which means that the $\pi$ overlap was also firmly enhanced compared to the isolated CO. Thus, the results are consistent with the known nucleophilic character of the carbon site. Indeed, the $\pi$ C—O character is enhanced in molecules such as $HCO^+$ where the $\pi$ orbital overlap is stronger than in CO. Indeed, for $HCO^+$, the quadrupolar polarization of 1.183 a.u. (see Table 4) appears very close to the $Q^+$-C-O system.

### *Insights from Coupled Study of Dipolar and Quadrupolar Polarization Contributions*

#### *Application to a Model of Aspartic HIV Protease Inhibitors*

Another intense discussion about the bonding nature can be found with the weak interaction between a tertiary amino group nitrogen and a formaldehyde group, i.e., N|···C=O.[51] Because this interaction could play a fundamental role in the activity of an original class of aspartic HIV protease inhibitors,[51f] a recent theoretical study[52] has cleared up the bonding scheme. According to this work, the model system studied here is a prototype of the NCO bond as illustrated in Figure 3.

The previous study has shown that the C—N and C—O distance are directly controlled by their environment (polarity and proticity of the medium) and two C—N distance regimes have been identified: a long regime ($d_{CN} > 2.5$ Å) where the interaction N—CO is mainly electrostatic and a short regime ($d_{CN} <$ 2.5 Å) stabilized by the medium. Table 4 presents the DEMEP analysis for the C—O bond of the formaldehyde group for two typical C—N distance regimes i.e., $r_{CN} = 3.00$ Å and $r_{CN} = 1.63$ Å.[52] Figure 3 illustrates the relative positions of these two molecules (long and short regimes) among other carbonyl



**Figure 3.** Bimolecular model of the N|-CO bond.

**Table 5.** Magnitudes of Local Dipole Contributions $|\mu|$, First Moments $|\mathbf{M}_1|$ and Second Moments $|\mathbf{M}_2|$ for Some Basins of Interest in Hydrocarbon Molecules $C^{(1)}H_3C^{(2)}H_2C^{(3)}H_2R$ and in the Main Chain $-C^{(2)}H(NH_2)C^{(1)}O^{(1)}O^{(2)}H$ of Amino Acids.

| Hydrocarbon[a] | V($C^{(1)}$, $C^{(2)}$)[b] | | | | V($C^{(2)}$, $C^{(3)}$) | | | | $|\mu_{CH3}|$[c] |
|---|---|---|---|---|---|---|---|---|---|
| | $\Delta M_0$[d] | $|\mathbf{M}_1|$ | $|\mathbf{M}_2|$ | $|\mu|$ | $\Delta M_0$[d] | $|\mathbf{M}_1|$ | $|\mathbf{M}_2|$ | $|\mu|$ | |
| Ethane | 0.00 | 0.000 | 0.302 | 2.65 | – | – | – | – | 1.516 |
| Propane | 0.02 | 0.005 | 0.307 | 2.68 | 0.00 | 0.005 | 0.303 | 6.87 | 1.542 |
| Butane | 0.02 | 0.008 | 0.311 | 2.69 | 0.02 | 0.003 | 0.314 | 6.97 | 1.553 |

| Amino acid[e] | V($C_1$, $O_1$) | | V($C_1$, $O_2$) | | V($C_2$, N) | | V(N) | | | V($O_2$) | | | $|\mu|$[f] |
|---|---|---|---|---|---|---|---|---|---|---|---|---|---|
| | $|\mathbf{M}_1|$ | $|\mathbf{M}_2|$ | $|\mathbf{M}_1|$ | $|\mathbf{M}_2|$ | $|\mathbf{M}_1|$ | $|\mathbf{M}_2|$ | $|\mathbf{M}_1|$ | $|\mathbf{M}_2|$ | $|\mu|$ | $|\mathbf{M}_1|$ | $|\mathbf{M}_2|$ | $|\mu|$ | |
| Glycine[g] | 0.255 | 1.249 | 0.052 | 0.257 | 0.183 | 0.166 | 0.952 | 0.125 | 11.6 | 3.308 | 2.446 | 11.6 | 0.50 (0.48) |
| | (0.247) | (1.221) | (0.050) | (0.270) | (0.207) | (0.177) | (1.055) | (0.100) | (12.0) | (2.955) | (2.136) | (11.5) | 0.48 (0.46) |
| Valine | 0.281 | 1.241 | 0.059 | 0.256 | 0.177 | 0.173 | 0.931 | 0.167 | 11.5 | 3.296 | 2.417 | 12.2 | 0.55 (0.55) |
| Tyrosine | 0.270 | 1.210 | 0.059 | 0.268 | 0.177 | 0.172 | 0.929 | 0.161 | 11,5 | 3.286 | 2.454 | 12,0 | 0.95 (0.92) |

[a]Hydrocarbon molecules optimized at the B3LYP/6-311G(3d) level of theory. The common origin of the axis system is chosen at the carbon atom of the methyl group.
[b]Bonding basin between the methyl group $C^{(1)}H_3$ and the nearest methylene group $C^{(2)}H_2$.
[c]Total molecular dipole of the amino acid in a.u. Values in parenthesis were obtained with the Gaussian 03 software.
[d]Relative basin population with respect to the ethane molecule.
[e]Amino acid molecules optimized at the B3LYP/6-31+G(d,p) level of theory. The common origin of the axis system is chosen at the carbon atom $C^{(1)}$.
[f]Total local dipole contributions of the methyl group including the bonding basin V($C^{(1)}$, $C^{(2)}$).
[g]The values given in parenthesis correspond to a single point calculation at the B3LYP/Aug-cc-pVTZ level of theory.

systems according to the quadrupolar polarization of the C—O bond.

These results show that the long distance regime is characterized by a strong value of the quadrupolar polarization magnitude (1.431 a.u.) and by a weak dipolar polarization magnitude of oxygen lone pair (0.944 a.u.), in agreement with the known $\pi$ character of the C—O bond and the $sp^2$ hybridization of the carbon atom. In addition, the dipole magnitude of the $H_2CO$ fragment (2.567 a.u.) is close to the value found for the isolated formaldehyde fragment (2.171 a.u.). In contrast, the short regime distance displays a weak CO quadrupolar polarization magnitude (0.423 a.u.) and a strong dipolar polarization magnitude of the oxygen lone pair (1.118 a.u.). Thus, the local dipole of the $H_2CO$ fragment appears enhanced at the short C—N distance ($|\mu| = 4.809$ D). In addition, CSOV calculations shows that the polarization energy is about −18.9 kcal/mol for the short regime compared to −0.2 kcal/mol for the long regime, in agreement with our DEMEP analysis. Finally, these results complement the previous study[52] explaining that the particular N—CO bond formation (long distance to short distance) is mainly driven by the enhancement of CO bond polarization induced by the effect of the near N lone pair.

### Application to the Cu—CO Bond

We conclude with a study the interaction between neutral copper and carbonyl molecule. Many theoretical studies as well as experimental (ref. 53 and references therein) have confirmed the original Dewar-Chatt-Duncanson donor-acceptor[54] orbital scheme of the M—CO bond where M is a transition metal. This picture rationalizes this interaction as a competitive charge transfer between the donation $CO(7\sigma)$ (Metal($d_\pi$) and the backdonation Metal($d_\pi$)($\pi^*$(CO) in the linear carbonyl complexes. The backdonation weakens the CO bond and explains the shift of the stretching frequencies of C—O bond to the lower values. In a recent work,[53] the ELF population analysis has confirmed this orbital scheme and backdonation was determined as the main process of the M—CO bond formation, donation remaining almost negligible. On the other hand, the ground state of the CuCO complex is known to have a bent geometry ($X^2A'$). It was demonstrated[53] that the bent structure allows a greater net charge transfer Cu → CO than the correlated linear structure ($^2\Sigma^+$). The DEMEP analysis should be able to confirm the scheme.

Table 4 shows the dipolar and quadrupolar polarization magnitudes for both geometries. In the linear CuCO structure, the quadrupolar polarization of the V(C, O) basin (0.841 a.u.) remains close to the value calculated for the isolated CO molecule (0.902 a.u.). In addition, the dipolar polarization magnitude of the oxygen lone pair is also pretty close to the observed value in the free carbonyl. This result means that the net charge transfer from the metal to the carbonyl Cu → CO for the linear geometry is weak since the $\pi$ bonding character remains very similar to the isolated CO molecule. In contrast, the bent geometry displays a slightly weaker bond quadrupolar polarization magnitude (0.784 a.u.). Thus, the $\pi$ character is weakened by a larger net charge transfer from the metal to the carbonyl. These results also confirm the earlier analyze[53] in which the charge transfer Cu → CO was found maximized for the bent geometry.

### *Transferability of ELF Moments: A Step Towards Force Fields*

Table 5 displays the magnitude of the local moments $M_0$, $|\mathbf{M}_1|$ and $|\mathbf{M}_2|$ for some basins of interest in three hydrocarbon molecules and in three amino acids.

Our results reflect the transferability properties of these moments. Indeed, the magnitudes of the bond local moments as well as the bond local dipoles are very stable in the related hydrocarbon compounds. Moreover, these values follow the trends already observed by Bader[12] with the AIM partition. Other examples of the transferability of the local moments can be found with amino acids such as the glycine, the valine and the tyrosine. Indeed, as shown in Table 5, the magnitude of the moments involved in the main chain —CH(NH$_2$)COOH appear reasonably stable. These last results are also in excellent agreement with comparable AIM studies.[11b,55] Moreover, such a transferability of these moments can be observed in Table 3 as the dipolar polarization $|\mathbf{M}_1|$ of the C—O bond is quite invariant in the CH$_2$X—COH compounds for any X substituant.

Table 5 also gives the topological moments obtained with the 6-31+G(d,p) and the AUG-CC-pVTZ basis sets for the glycine molecule. The magnitude of the topological moments values appear comparable with these two different basis sets. In contrast to the well known basis set dependence of the Mulliken partition, the topological partition appears then less sensitive to basis sets in agreement with previous studies.[11,48]

Such encouraging results show that a direct use of these topological moments is possible for the design of advanced force fields. Indeed, the general mathematical framework defining the local frames permitting the rotation of any nonatomic centers moments, such as lone pairs, is already available. It has been extensively tested in the framework of the gaussian electrostatic model (GEM).[7,56,57] As numerical evaluation of hermites Gaussian densities is now possible,[10] we will present a coupled DEMEP/GEM approach in a forthcoming paper (Cisneros et al., unpublished observations).

## Conclusion

In this work, we have investigated the evaluation of local electrostatic moment values by means of the topological analysis of the ELF function. Results show that this approach is able to reproduce molecular dipole from integrations over ELF basins and to evaluate local moments located on lone pairs, $\sigma$ bonds and $\pi$ systems. As the DEMEP analysis has been successfully applied to a large set of molecules, local dipoles have been shown to be useful to study lone pairs and intermolecular interactions. For example, local bond second moments provide insights about the nature of chemical bonding enabling to discuss $\sigma$–$\pi$ mixing and bond multiplicity, aromaticity, and ligand effects. Moreover, we have shown that the dipolar polarization of lone pairs is clearly linked to the chemical reactivity. Our results have also shown that local dipoles are dominated by the charge transfer contributions in the case of bonds. Our DEMEP analysis appears as useful tool to observe the fluctuations of the $\pi$ character of the CO bond when subjected to intramolecular interactions in the case of the weak N—CO bond. The approach showed clearly a weakening of the bond and could find applications in the theoretical study of many biological systems. Although no partition of space can be considered as unique or perfect, we believe that the DEMEP analysis has the potential to be a useful tool for the rationalization of electronic structures.

Future works will focus on the applicability of this new potentiality of the ELF topological analysis to quantum chemistry and to reactivity. The DEMEP approach will also be coupled to density fitting[58,59] to be applied to molecular modeling in the framework of next generation GEM[7,10,56,57] force field. Indeed, the approach based on electron density offers the possibility to extract distributed multipoles and is able to treat non atomic centers.

## References

1. Stone, A. J.; Aderton, M. Chem Phys Lett 1981, 83, 233.
2. Stone, A. J.; Aderton, M. Mol Phys 1985, 56, 1047.
3. Stone, A. J. J Chem Theor Comput 2005, 1, 1128.
4. (a) Claverie, P. Localization and Delocalization in Quantum Chemistry, Vol. 2; Chalvet, O.; Daudel, R.; Diner, S.; Malrieu, J. P., Eds.; Reidel: Dordrecht, 1976; p. 127; (b) Vigné-Maeder, F.; Claverie, P. J Chem Phys 1988, 88, 4934.
5. Volkov, A.; Coppens, P. J Comput Chem 2004, 25, 921.
6. (a) Soderhjelm, P.; Krogh, J. W.; Karlström, G.; Ryde, U.; Lindh, R. J Comput Chem 2007, 28, 1083; (b) Gagliardi, L.; Lindh, R., Karlström, G. J Chem Phys 2004, 121, 4494; (c) Holt, A.; Karlström, G.; Lindh, R. J Chem Phys Lett 2007, 436, 297.
7. Cisneros, G. A.; Piquemal, J.-P.; Darden, T. A. J Chem Phys 2006, 125, 184101.
8. Williams, D. E. Rev Comput Chem 1991, 2, 219.
9. Chipot, C.; Angyan, J. G.; Millot, C. Mol Phys 1998, 94, 881.
10. Cisneros, G. A.; Elking, D.; Piquemal, J.-P.; Darden, T. A. J Phys Chem A, 111, 12049.
11. (a) Bader, R. F. W. Atoms in Molecules: A Quantum Theory; Oxford University Press: Oxford, 1990; (b) Matta, C. F.; Boyd, R. J. The Quantum Theory of Atoms in Molecules: From Solid State to DNA and Drug Design; Wiley-VCH: Weinheim, 2007.
12. (a) Bader, R. F. W.; Bedall, P. M.; Cade, P. E. J Am Chem Soc 1971, 93, 3095; (b) Bader, R. F. W.; Larouche, A.; Gatti, C.; Caroll, M. T.; Dougall, P. J.; Wiberg, K. B. J Chem Phys 1987, 87, 1142.
13. (a) Popelier, P. L. A. Atoms in Molecules: An Introduction; Prentice-Hall: Harlow, U. K., 2000; (b) Popelier, P. L. A. Mol Phys 1996, 87, 1169; (c) Popelier, P. L. A.; Stone, A. J. Mol. Phys. 1994, 82 411; (d) Popelier, P. L. A.; Joubert, L.; Kosov, D. S. J Phys Chem A 2001, 105, 8254.
14. Millot, C.; Stone, A. J Mol Phys 1992, 77, 439.
15. Piquemal, J.-P.; Chevreau, H.; Gresh, N. J Chem Theory Comput 2007, 3, 824.
16. (a) Liem, S. Y.; Popelier, P. L. A.; Leslie, M. Int J Quant Chem 2004, 9, 685; (b) Devereux, M.; Popelier, P. L. A. J Phys Chem A 2007, 111, 1536; (c) Liem, S. Y.; Popelier, P. L. A. J Chem Phys 2003, 119, 4560.

17. Ren, P.; Ponder, J. W. J Phys Chem B 2003, 107, 5933.

18. Piquemal, J.-P.; Gresh, N.; Giessner-Prettre, C. J. Phys Chem A 2003, 107, 10353.

19. Piquemal, J.-P.; Perera, L.; Cisneros, G. A.; Ren, P.; Pedersen, L. G.; Darden, T. A. J Chem Phys 2006, 125, 054511.

20. (a) Piquemal, J.-P.; Procacci, P.; Chelli, R.; Gresh, N. J Phys Chem A 2007, 111, 8170; (b) Frenking, G.; Loschen, C.; Krapp, A.; Fau; S.; Strauss, S. H. J Comput Chem 2006, 28, 117.

21. Becke, A. D.; Edgecombe, K. E. J Chem Phys 1990, 92, 5397.

22. Silvi, B.; Savin, A. Nature 1994, 371, 683.

23. Savin, A.; Nesper, R.; Wengert, S.; Fässler, T. F. Angew Chem Int Ed Eng 1997, 36, 1809.

24. Silvi, B. J Phys Chem A 2003, 107, 3081.

25. Fuster, F.; Sevin, A.; Silvi, B. J Phys Chem A 2000, 104, 852.

26. Piquemal, J.-P.; Maddaluno, J.; Silvi, B.; Giessner-Prettre, C. New J Chem 2003, 27, 909.

27. Polo, V.; Andres, J.; Castillo, R.; Berski, S.; Silvi, B. Chem Eur J 2004, 10, 5165.

28. Pilmé, J.; Silvi, B.; Alikhani, E. A. J Phys Chem A 2005, 109, 10028.

29. Piquemal, J.-P.; Pilmé, J. J Mol Struct (Theochem) 2006, 764, 77.

30. Gourlaouen, C.; Piquemal, J.-P.; Parisel, O. J Chem Phys 2006, 124, 174311.

31. (a) Gourlaouen, C.; Parisel, O. Angew Chem Int Ed Eng 2007, 46, 553; (b) Gourlaouen, C.; Gérard, H.; Piquemal, J.-P.; Parisel, O. Chem Eur J (in press) DOI: 10.1002/chem. 200701265.

32. Poater, J.; Duran, M.; Solà, M.; Silvi, B. Chem Rev 2005, 105, 3911.

33. Berski, S.; Andrés, J.; Silvi, B.; Domingo, L. R. J Phys Chem A 2006, 110, 13939.

34. (a) Gillespie, R. J.; Nyholm, R. S. Q. Rev Chem Soc 1957, 11, 339. (b) Gillespie, R. J. Molecular Geometry; Van Nostrand Reinhold: London, 1972.

35. (a) Noury, S.; Silvi, B.; Gillespie, R. J. Inorg Chem 2002, 41, 2164; (b) Pilmé, J.; Robinson, E. A.; Gillespie, R. J. Inorg Chem 2006, 45, 6198.

36. Stone, A. J. The Theory of Intermolecular Forces; Oxford University Press: UK, 2000.

37. Coulson, C. A. Trans Faraday Soc 1942, 38, 433.

38. Lee, C.; Yang, W.; Parr, R. G. Phys Rev B 1988, 37, 785.

39. Becke, A. D. J Chem Phys 1993, 98, 5648.

40. Gaussian 03, Revision B. 02. Frisch, M. J.; Trucks, G. W.; Schlegel, H. B.; Scuseria, G. E.; Robb, M. A.; Cheeseman, J. R.; Montgomery, J. A., Jr.; Vreven, T.; Kudin, K. N.; Burant, J. C.; Millam, J. M.; Iyengar, S. S.; Tomasi, J.; Barone, V.; Mennucci, B.; Cossi, M.; Scalmani, G.; Rega, N.; Petersson, G. A.; Nakatsuji, H.; Hada, M.; Ehara, M.; Toyota, K.; Fukuda, R.; Hasegawa, J.; Ishida, M.; Nakajima, T.; Honda, Y.; Kitao, O.; Nakai, H.; Klene, M.; Li, X.; Knox, J. E.; Hratchian, H. P.; Cross, J. B.; Bakken, V.; Adamo, C.; Jaramillo, J.; Gomperts, R.; Stratmann, R. E.; Yazyev, O.; Austin, A. J.; Cammi, R.; Pomelli, C.; Ochterski, J. W.; Ayala, P. Y.; Morokuma, K.; Voth, G. A.; Salvador, P.; Dannenberg, J. J.; Zakrzewski, V. G.; Dapprich, S.; Daniels, A. D.; Strain, M. C.; Farkas, O.; Malick, D. K.; Rabuck, A. D.; Raghavachari, K.; Foresman, J. B.; Ortiz, J. V.;
Cui, Q.; Baboul, A. G.; Clifford, S.; Cioslowski, J.; Stefanov, B. B.; Liu, G.; Liashenko, A.; Piskorz, P.; Komaromi, I.; Martin, R. L.; Fox, D. J.; Keith, T.; Al-Laham, M. A.; Peng, C. Y.; Nanayakkara, A.; Challacombe, M.; Gill, P. M. W.; Johnson, B.; Chen, W.; Wong, M. W.; Gonzalez, C.; Pople, J. A. Gaussian, Inc., Pittsburgh PA, 2004.

41. (a) Noury, S.; Krokidis, X.; Fuster, F.; Silvi, B. Comput Chem 1999, 23, 597; (b) The modified TopMod program (named TopChem) is available upon request. See the following website for details: Available at: http://www.lct.jussieu.fr/pagesperso/pilme

42. Bagus, P. S.; Illas, F. J. Chem Phys 1992, 96, 8962.

43. Piquemal, J.-P.; Marquez, A.; Parisel, O.; Giessner-Prettre, C. J Comput Chem 2005, 26, 1052.

44. Dupuis, M.; Marquez, A.; Davidson, E. R. HONDO 95.3 QCPE; Indiana University: Bloomington, IN, 1995.

45. Morokuma, K.; Pedersen, L. G. J Chem Phys 1968, 42, 3875.

46. (a) Tschumper, G. S.; Leininger, M. L.; Hoffman, B. C.; Valeev, E. F.; Schaefer, H. F.; Quack, M. J Chem Phys 2002, 116, 690; (b) Huang, X.; Bastiaan, J.; Braams, A.; Bowman, J. M. J Phys Chem A 2006, 110, 445.

47. Gatti, C.; Silvi, B.; Colonna, F. Chem Phys Lett 1995, 247, 135.

48. Slee, T.; Larouche, A.; Bader, R. F. W. J Phys Chem 1988, 92, 6219.

49. van Mourik, T.; Karamertzanis, P. G.; Price, S. L. J Phys Chem A 2006, 110, 8.

50. (a) Frenking, G.; Fröhlich, N. Chem Rev 2000, 100, 717; (b) Frenking, G. J Organomet Chem 2001, 635, 9; (c) Frenking, G.; Wichmann, K.; Fröhlich, N.; Loschen, C.; Lein, M.; Frunzke, J.; Rayón, V. M. Coord Chem Rev 2003, 55, 238.

51. (a) Kermack, W. O.; Robinson, R. J. J Chem Soc 1922, 121, 427; (b) Bürgi, H. B.; Dunitz, J. D. Acc Chem Res 1983, 16, 153; (c) Studer, M.; Blaser, H.-U.; Exner, C. Adv Synth Catal 2003, 1/2, 45; (d) Griffith, R.; Bremner, J. B. J Comput Aided Mol Des 1999, 13, 69; (e) Leonard, N. J. Rec Chem Prog 1956, 17, 243 and references there in Acc Chem Res 1979, 12, 423 and references there in; (f) Gautier, A.; Pitrat, D.; Hasserodt, J. Bioorg Med Chem 2006, 14, 3835.

52. Pilmé, J.; Berthoumieux, H.; Fleurat-Lessard, P.; Robert, V. Chem Eur J 2007, 13, 5388.

53. Pilmé, J.; Alikhani, M. E.; Silvi, B. J Phys Chem A 2003, 107, 4506.

54. (a) Dewar, M. J. S. Bull Soc Chim Fr 1951, 18, C79; (b) Chatt, J.; Duncanson, L. A. J Am Chem Soc 1953, 2939.

55. (a) Matta, C. F.; Bader, R. F. W. Proteins 2000, 40, 310; (b) Matta, C. F.; Bader, R. F. W. Proteins 2002, 48, 519; (c) Matta, C. F.; Bader, R. F. W. Proteins 2003, 52, 360; (d) Bader, R. F. W.; Matta, C. F. Int J Quantum Chem 2001, 85, 592.

56. Piquemal, J.-P.; Cisneros, G. A.; Reinhardt, P.; Gresh, N.; Darden, T. A. J Chem Phys 2006, 124, 104101.

57. Gresh, N.; Cisneros, G. A.; Darden, T. A.; Piquemal, J.-P. J Chem Theory Comput 2007, 3, 1960.

58. Dunlap, B. I.; Connolly, J. W. D.; Sabin, J. R. J Chem Phys 1979, 71, 4993.

59. Cisneros, G. A; Piquemal, J.-P.; Darden, T. A. J Chem Phys 2005, 123, 044109.